Some Factors and Effects on Thermally Structural Changes of Lattice for Cyanide-Bridged Bimetallic Assemblies of Cu(II)

Takashiro Akitsu*, Mao Ohwa, Yuki Endo, Satoru Sonoki, Yoshikazu Aritake, and Yusuke Kimoto

Department of Chemistry, Faculty of Science, Tokyo University of Science, 1-3 Kagurazaka, Shinjuku-ku, Tokyo 162-8601, Japan

Abstract: In order to understand novel structural features of crystal packing of $[CuL_2][Ni(CN)_4]\cdot 2H_2O$ (L = (1*R*,2*R*)-1,2-diaminocyclohexane), we have investigated temperature effect, metal-size effect, and isotope effect and their temperature dependence (100-300 K) with synchrotron powder X-ray diffraction (XRD) for (1) $[CuL_2][M(CN)_4]\cdot 2H_2O$ (M=Pd, Pt), (2) $[CuL'_2][M(CN)_4]$ (M=Ni, Pd, and Pt; L' = *N*-ethylethylenediamine), and (3) $[CuL''_2][M(CN)_6]\cdot nH_2O$ (L'' =(1*S*,2*S*)-1,2-dimethylcyclohexanediamine. M=Cr, Co, and Fe; isotopes of H_2O are $^1H(H)$, $^2H(D)$, and $^{18}O(O)$, respectively). The effect of the factors of (1) (temperature difference of 200 K) is comparable to metal size for the system of (1). Combinatorial preparation of (2) gave rise to the most stable Pd(II) complexes predominantly. Isotope effect of water molecules resulted in little structural changes of lattice for (3).

Keywords: Powder X-ray diffraction, lattice distortion, temperature, copper, isotope.

INTRODUCTION

Some flexible frameworks of cyanide-bridged bimetallic assemblies exhibit novel structural crystallographic features. For example, guest-dependent reversible structural transformation due to dehydration by heating and hydration has been reported for chiral coordination polymers [1-3]. Guest-dependent negative thermal expansion behavior, showing contraction of cell volume and/or length of axes on heating, can be observed for certain Prussian blue analogues [4, 5], which are dependent on lattice dynamic effect of nanoporous frameworks. Furthermore, some coordination polymers exhibit colossal positive and negative thermal expansion [6], in particular, metallophilic interaction d^{10} closed-shell interactions may be suitable flexible building blocks for the frameworks of these crystalline materials [7].

We have investigated structural flexibility of $3d^9$ copper(II) complexes [8] and their cyanide-bridged bimetallic assemblies [9] due to Jahn-Teller distortion [10, 11]. Herein we report on variable temperature XRD and attempt of preparation bimetallic assemblies potentially having long semi-coordination bonds [12, 13] and related complexes [14, 15]. In order to understand novel structural features of crystal packing of $[CuL_2][Ni(CN)_4]\cdot 2H_2O$ (L = (1*R*,2*R*)-1,2-diaminocyclohexane), we have investigated temperature effect, metal-size effect, and isotope effect and their temperature dependence (100-300 K) with synchrotron powder X-ray diffraction (XRD) for (1) $[CuL_2][M(CN)_4]\cdot 2H_2O$ (M=Pd, Pt), (2) $[CuL'_2][M(CN)_4]$ (M=Ni, Pd, or Pt; L' = *N*-ethylethylenediamine), and (3) $[CuL''_2]_3[M(CN)_6]_2\cdot nH_2O$ (L'' =(1*S*,2*S*)-1,2-dimethylcyclohexanediamine. M=Cr, Co, and Fe; isotopes of H_2O are $^1H(H)$, $^2H(D)$, and $^{18}O(O)$, respectively). The purpose is the present study is not completely determination of crystal structures from powder XRD data but experimental benchmark tests for some effects of chemical modifications on thermally structural changes, which have been never carried out actually.

MATERIALS AND METHODOLOGY

Preparations

$[CuL_2][M(CN)_4]\cdot 2H_2O$ [12, 13] and $[CuL'_2][M(CN)_4]$ [14, 15] were prepared according to the literature methods. Combinatorial preparation of the system (2) by using different $[M(CN)_4]^{2-}$ precursors was carried out and characterized XPS and XRD. Total 9 compounds of (3), $[CuL''_2]_3[M(CN)_6]_2\cdot nH_2O$, Cr-H, Cr-D, Cr-O, Co-H, Co-D, Co-O, Fe-H, Fe-D, and Fe-O, were prepared in similar way to the analogous compounds [9] by employing the corresponding amine ligands (L''') and water containing isotope atoms.

Physical Measurements

X-ray photoelectron spectra (XPS) were recorded with a JEOL JPS-9010MC at 298 K. Powder samples were pressed as pellets and put under UHV to reach the 10^{-8} Pa range. The nonmonochromatized Mg Kα source was used at 10 kV and 10 mA, as a flood gun to compensate for the nonconductive samples. The binding energy of the spectra was calibrated in relation to the C 1s binging energy (284.0 eV), which was applied as an internal standard. Powder XRD patterns were also measured by using synchrotron radiation beamline at KEK-PF BL-8B with 8 keV (λ = 1.54184 Å) under variable temperature apparatus of nitrogen stream equipped with a

*Address correspondence to this author at the Department of Chemistry, Faculty of Science, Tokyo University of Science, 1-3 Kagurazaka, Shinjuku-ku, Tokyo 162-8601, Japan; Tel: +81-3-5228-8271; Fax; +81-3-5261-4631; E-mail: akitsu@rs.kagu.tus.ac.jp

1874-8465/11 2011 Bentham Open

RIGAKU imaging plate. All the samples were measured for 3 min and constant ring current (440 mA).

RESULTS AND DISCUSSION

Figs. (**1** and **2**) exhibit variable temperature XRD patterns for $[CuL_2][Pd(CN)_4]\cdot 2H_2O$ and $[CuL_2][Pt(CN)_4]\cdot 2H_2O$, respectively. The predominant peaks of (0, 2, 1), (2, 0, -1), and (1, 0, 0) appear around 2θ = 16.4, 18.6, and 9.6 degrees, respectively. Both complexes exhibited usual positive thermal expansion upon heating [16]. The d-values of (0, 2, 1), (2, 0, -1), and (1, 0, 0) peaks at 300 K are 5.42, 4.80, and 9.21 Å and the difference between 300 K and 100 K are 0.029, 0.000, and 0.000 Å for $[CuL_2][Pd(CN)_4]\cdot 2H_2O$. The corresponding values for $[CuL_2][Pt(CN)_4]\cdot 2H_2O$ are 5.40, 4.78, and 9.24 Å and the difference between 300 K and 100 K are 0.028, 0.000, and 0.006 Å, respectively.

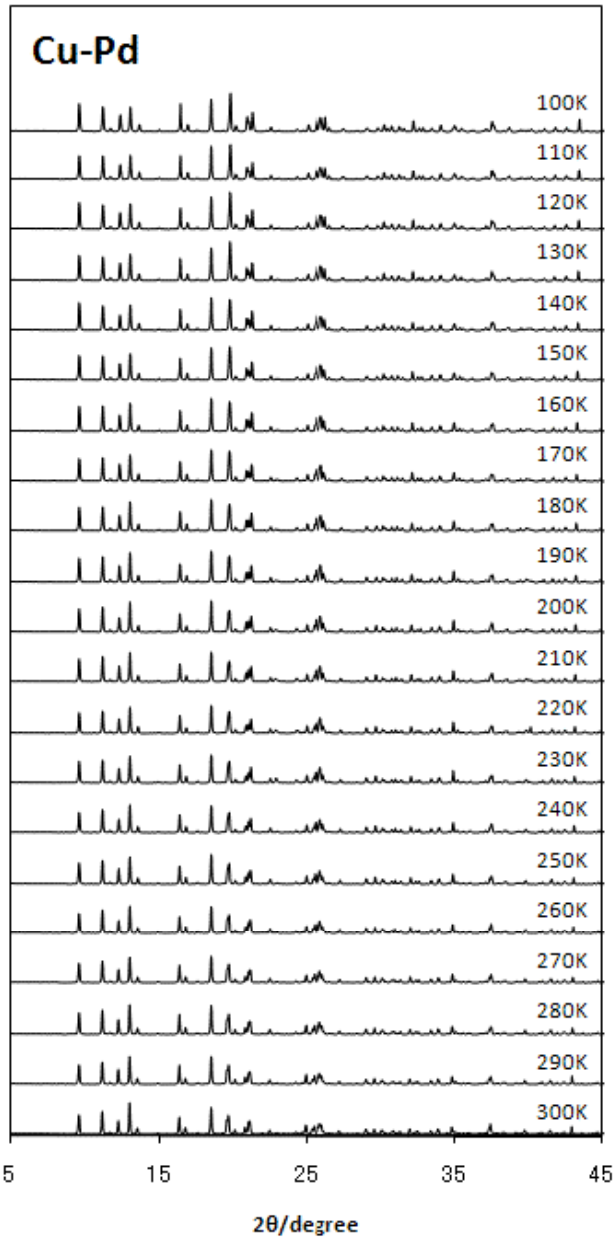

Fig. (1). Powder XRD patterns for $[CuL_2][Pd(CN)_4]\cdot 2H_2O$ obtained with synchrotron radiation (λ = 1.54184 Å) at 100-300 K.

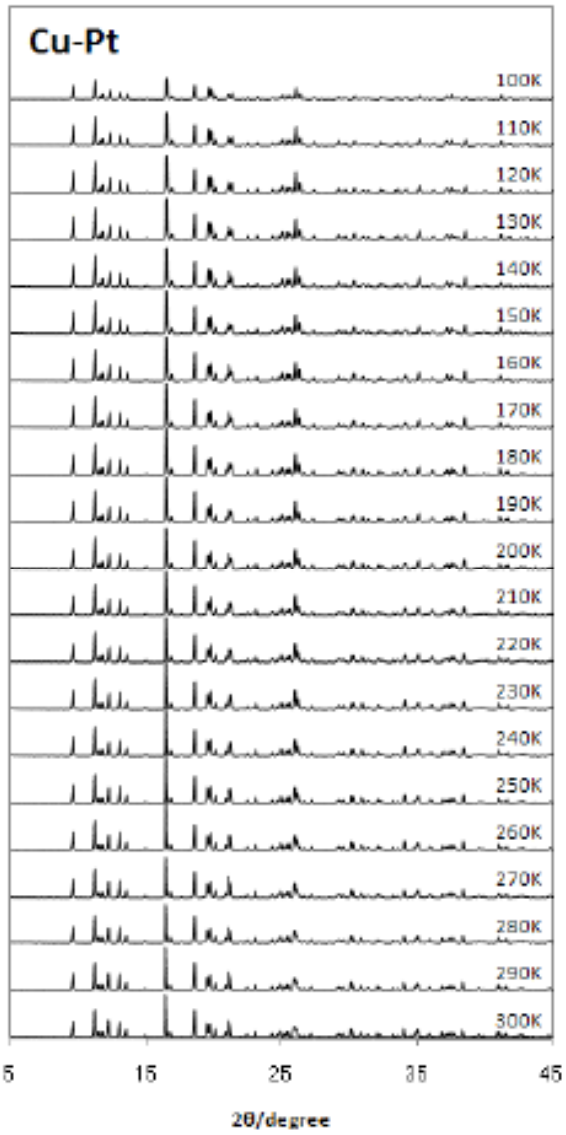

Fig. (2). Powder XRD patterns for $[CuL_2][Pt(CN)_4]\cdot 2H_2O$ obtained with synchrotron radiation (λ = 1.54184 Å) at 100-300 K.

On the other hand, the difference due to metal-substitution (Pd and Pt) at 300 K are 0.02, 0.02, and 0.03 Å for (0, 2, 1), (2, 0, -1), and (1, 0, 0) peaks, respectively. It should be noted that structural differences in d-values attributed to temperature difference (300 K and 100 K) were comparable to that attributed to metal- substitution (Pd and Pt) for these complexes. In this context, it may be interesting that $[CuL_2][Pd_{1-x}Pt_x(CN)_4]\cdot 2H_2O$ ($0 < x < 1$) may be a promising material which indicate novel thermal expansion behavior as functions of temperature and composition (x), because $[CuL_2][Pd(CN)_4]\cdot 2H_2O$ and $[CuL_2][Pt(CN)_4]\cdot 2H_2O$ crystallize isostructurally [12, 13]. However, in the systematic studies of cyanide-bridged bimetallic assemblies, we have not obtained such complexes so far.

We have prepared precursors as aqueous solutions of precursors under two conditions: <condition 1> $[CuL_2(H_2O)_2]^{2+}$ (9.03 mg, 0.02 mmol) and both $K_2[Pd(CN)_4]$ (2.29 mg, 0.01 mmol), and $K_2[Pt(CN)_4]$ (4.31 mg, 0.01 mmol), <condition 2> $[CuL_2(H_2O)_2]^{2+}$ (4.51 mg, 0.01 mmol) and both $K_2[Pd(CN)_4]$ (2.89 mg, 0.1 mmol), and $K_2[Pt(CN)_4]$

(2.89 mg, 0.005 mmol) to give rise to a blue single crystal. According to XPS results showing only Pd $3d_{3/2}$ and Pd $3d_{5/2}$ peaks around 340 eV , only $[CuL_2][Pd(CN)_4]\cdot 2H_2O$ precipitated for both conditions.

In order to prepare such mixed-metal bimetallic assemblies, we also examined the related cyanide-bridged complexes, $[CuL'_2][M(CN)_4]$ (M = Ni, Pd, Pt). We have prepared by using aqueous solutions of precursors of three or two components; <condition 1> $[CuL'_2(H_2O)_2]^{2+}$ (36.3 mg, 0.1 mmol) and $K_2[Ni(CN)_4]$ (8.62 mg, 0.033 mmol), $K_2[Pd(CN)_4]$ (9.61 mg, 0.033 mmol), and $K_2[Pt(CN)_4]$ (13.9 mg, 0.033 mmol) <condition 2> $[CuL'_2(H_2O)_2]^{2+}$ (36.4 mg, 0.1 mmol) and both $K_2[Pd(CN)_4]$ (14.0 mg, 0.05 mmol), and $K_2[Pt(CN)_4]$ (21.1 mg, 0.05 mmol) to give rise to a blue single crystal. According to XPS results showing only Pd $3d_{3/2}$ and Pd $3d_{5/2}$ peaks around 340 eV, only $[CuL'_2][Pd(CN)_4]\cdot 2H_2O$ precipitates were obtained for both conditions. Figs. (**3** and **4**) show the corresponding XRD patterns at 300 K and 100 K, which indicate single component patterns surely.

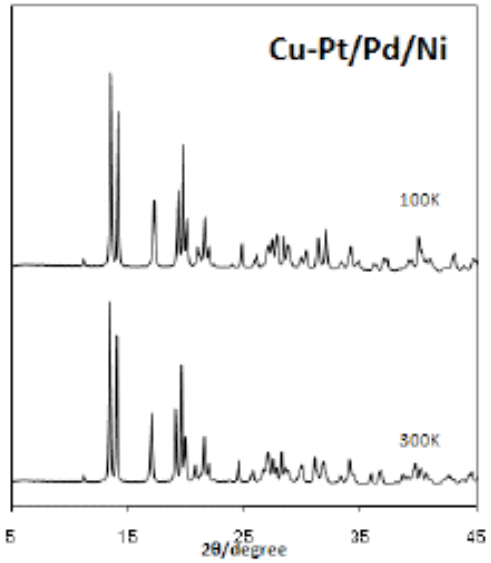

Fig. (3). Powder XRD patterns for $[CuL'_2][Pd(CN)_4]$ (prepared as mixture of Ni/Pd/Ni) obtained with synchrotron radiation (λ = 1.54184 Å) at 100 and 300 K.

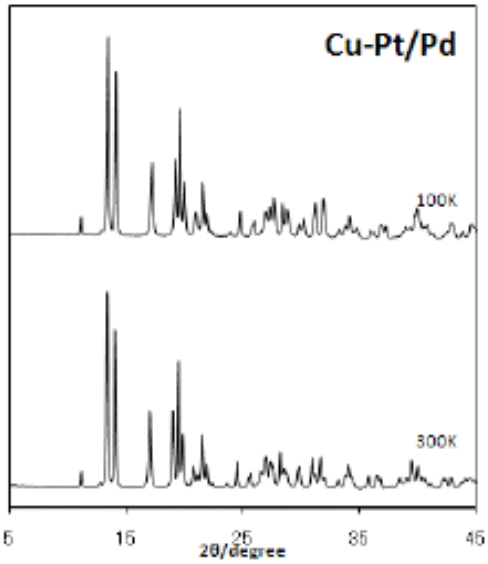

Fig. (4). Powder XRD patterns for $[CuL'_2][Pd(CN)_4]$ (prepared as mixture of Pd/Ni) obtained with synchrotron radiation (λ = 1.54184 Å) at 100 and 300 K.

By the way, Figs. (**5-7**) exhibit variable temperature XRD patterns for $[CuL''_2]_3[M(CN)_6]_2\cdot nH_2O$ (whose water are substituted H, D, and O isotopes), respectively. Among these 9 isostructural crystals, metal substitution (M=Cr, Co, and Fe) results in slight structural difference similar to ion size difference between Pd and Pt as mentioned above. Although strength of hydrogen bonds should be expected to vary depending on isotopes, isotope substitution resulted in little structural difference in XRD patterns examined.

Temperature dependence of XRD patterns of $[CuL''_2]_3[M(CN)_6]_2\cdot nH_2O$ clearly indicates that their crystal lattice exhibits isotropic normal (positive) thermal expansion behavior (even only several points are recorded) for $[CuL''_2]_3[Fe(CN)_6]_2\cdot nH_2O$ (H) (Fig. **8**). In this way, isotope effect may emerge not as lattice behavior but also specific interatomic distances. Therefore, thermally-induced structural changes of crystal lattice constants and each bond distance may be observed separately for hydrogen bonded systems or a certain packing systems involving considerably anisotropic chemical bonds.

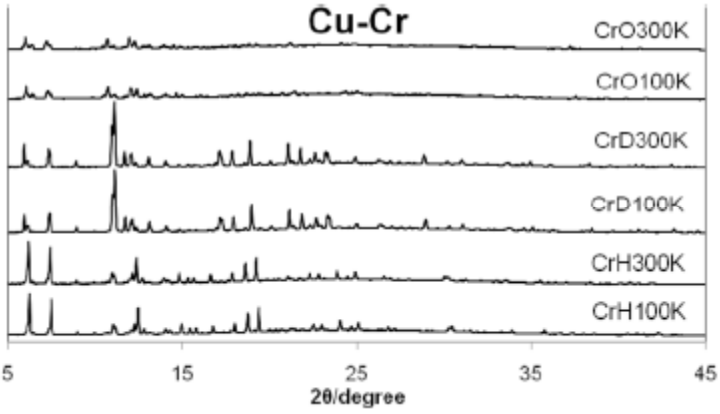

Fig. (5). Powder XRD patterns for $[CuL''_2][Cr(CN)_6]\cdot nH_2O$ (H, D, and O) obtained with synchrotron radiation (λ = 1.54184 Å) at 100 and 300 K.

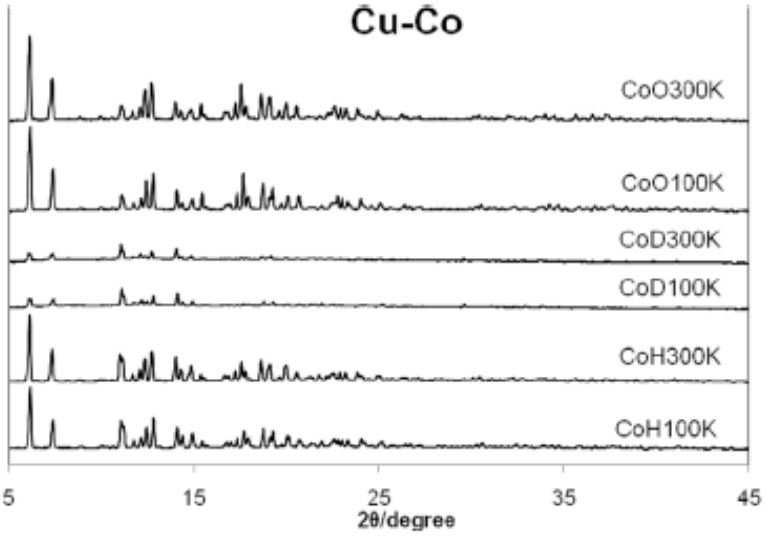

Fig. (6). Powder XRD patterns for $[CuL''_2][Co(CN)_6]\cdot nH_2O$ (H, D, and O) obtained with synchrotron radiation (λ = 1.54184 Å) at 100 and 300 K.

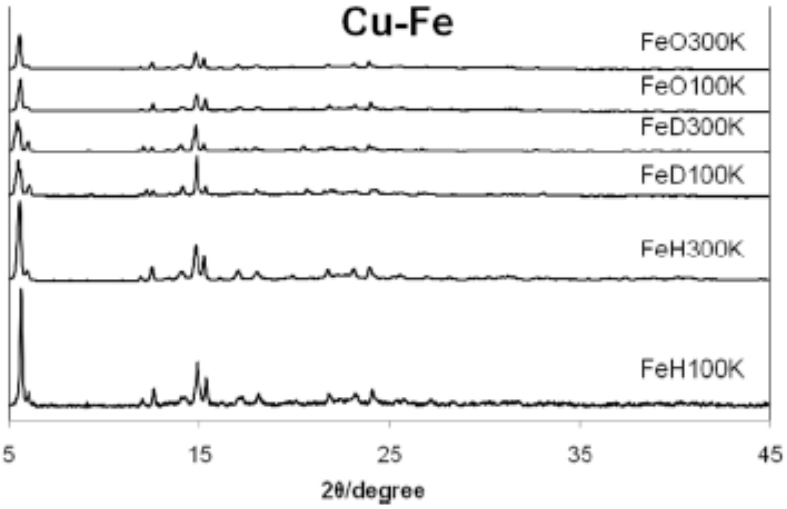

Fig. (7). Powder XRD patterns for $[CuL''_2][Fe(CN)_6]\cdot nH_2O$ (H, D, and O) obtained with synchrotron radiation (λ = 1.54184 Å) at 100 and 300 K.

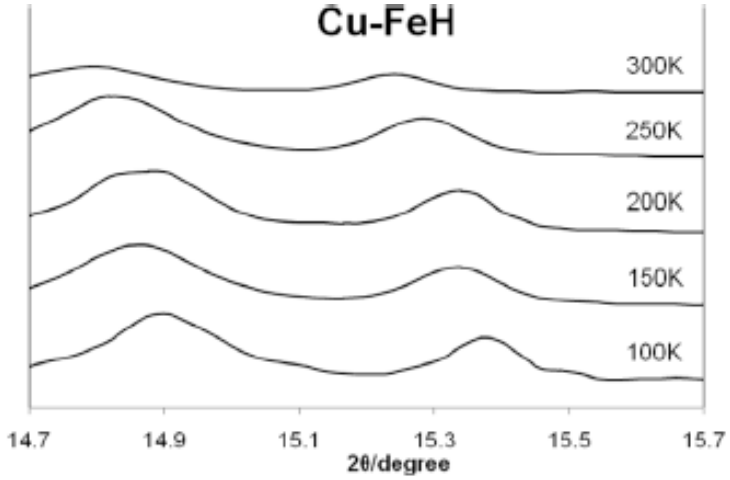

Fig. (8). Powder XRD patterns for $[CuL''_2][Fe(CN)_6]\cdot nH_2O$ (H) obtained with synchrotron radiation (λ = 1.54184 Å) at 100-300 K.

CONCLUSION

In order to design new materials to exhibit novel thermal expansion behavior, we examined temperature dependence of structural features for some cyanide-bridged bimetallic assemblies. The effect of the factors (1), 200 K temperature, was comparable to metal size for the system of (1). Combinatorial preparation of (2) gave rise to the most stable Pd(II) complexes. Isotope effect exhibited little effects on structural changes of lattice for (3). It was found that structural differences in d-values attributed to temperature difference (300 K and 100 K) are comparable to that attributed to metal- substitution (Pd and Pt) for these complexes. In this way one can conclude that at present it is easy to obtain middle size of $[CuA_2][Pd(CN)_4]\cdot 2H_2O$ and difficult to prepare $[CuA_2][Pd_{1-x}Pt_x(CN)_4]\cdot 2H_2O$ ($0 < x < 1$) type cyanide-bridged bimetallic assemblies. It is possible that expected thermally-induced structural changes of crystal lattice constants and each bond distance may be observed separately.

ACKNOWLEDGEMENTS

X-ray crystallography using synchrotron radiation was carried out at KEK-PF BL-8B (2008G526).

REFERENCES

[1] Sereda O, Stoeckli-Evans H, Dolomanov O, Filinchuk Y, Pattison P. Transformation of a chiral nanoporus bimitallic cyano-bridged framework triggered by dehydration/rehydration. Crystal Growth Des 2009; 9: 3168-78.

[2] Sereda O, Neels A, Stoeckli F, Stoeckli-Evans H, Filinchuk Y. Sponge-like reversible transformation of a bimetallic cyanometallate polymer. Crystal Growth Des 2008; 8: 2307-11.

[3] Sereda O, Neels A, Stoeckli F, Stoeckli-Evans H. Chiral bimetallic assemblies and coordination polymers based on tetracyanonickelate: a striking reversible structural transformation. Crystal Growth Des 2008; 8: 3380-4.

[4] Goodwin AL, Chapman KW, Kepert CJ. Guest-dependent negative thermal expansion in nanoporous prussian blue analogues $M^{II}Pt^{IV}(CN)_6\cdot x\{H_2O\}$ ($0 < x < 2$; M = Zn, Cd). J Am Chem Soc 2005; 127: 17980-1.

[5] Goodwin AL, Kennedy BJ, Kepert CJ. Thermal expansion matching *via* framework flexibility in zinc dicyanomellates. J Am Chem Soc 2009; 131: 6334.

[6] Goodwin AL, Calleja M, Conterio MJ, *et al*. Colossal positive and negative thermal expansion in the framework material $Ag_3[Co(CN)_6]$. Science 2008; 319: 794-7.

[7] Korcok JL, Katz MJ, Leznoff DB. Impact of metallophilicity on "colossal" positive and negative thermal expansion in a series of isostructural dicyanometallate coordination polymers. J Am Chem Soc 2009; 131: 4866-71.

[8] Akitsu T, Einaga Y. Thermal and photo-responsibiliry of axial semi-coordination bonds in Copper(II) complex. Bull Chem Soc Jpn 2004; 77: 763-4.

[9] Akitsu T, Einaga Y, Yoza K. Thermally-accessible lattice strain and local pseudo jahn-teller distortion in various dimensional Cu^{II}-M^{III} bimetallic cyanidE-bridged assemblies. Open Inorg Chem J 2008; 2: 1-10.

[10] Falvello LR. Jahn-Teller effects in solid-state co-ordination chemistry. J Chem Soc Dalton Trans 1997; 4463-76.

[11] Halcrow MA. Interpreting and controlling the structures of six-coordinate copper(II) centres – When is a compression really a compression? Dalton Trans 2003; 4375-84.

[12] Akitsu T, Einaga Y. Extremely long axial Cu-N bonds in chiral one-dimensional zigzag cyanide-bridged Cu^{II}-Ni^{II} and Cu^{II}-Pt^{II} bimetallic assemblies. Inorg Chem 2006; 45: 9826-33.

[13] Akitsu T, Einaga Y. Tuning of electronic properties of one-dimensional cyano-bridged Cu^{II}-Ni^{II}, Cu^{II}-Pd^{II}, and Cu^{II}-Pt^{II} bimetallic assemblies by stereochemistry of ligands. Inorg Chim Acta 2008; 361: 36-42.

[14] Akitsu T, Einaga Y. Structures, magnetic properties, and XPS of one-dimensional cyanide-bridged Cu^{II}-Ni^{II}/Pt^{II} bimetallic assembly complexes. Inorg Chim Acta 2007; 360: 497-505.

[15] Akitsu T, Endo Y. The one-dimensional chain structure of $Cu(N\text{-}Eten)_2Pd(CN)_4$ (N-Eten = N-ethylethylenediamine). Acta Cryst E 2009; 65: m406-m7.

[16] Akitsu T, Sano K. Analogy of van't hoff relationship for thermally-accessible lattice strain of Copper(II) complex. Netsu Sokutei 2009; 36: 244-6.

Received: May 18, 2010 Revised: January 04, 2011 Accepted: January 04, 2011